

A New Investigation of Prey-Predator Interactions Among Bacterial Species and Protozoa Under Atangana-Baleanu-Caputo Derivative

Mohammad Partohaghighi¹, Mustafa Inc^{2,3,4}, Sania Qureshi^{5,6}, Evren Hincal^{6,7,*}, Asif Ali Shaikh⁵ and Nezihal Gokbulut^{6,7}

¹ Department of Mathematics, Clarkson University, Potsdam, NY 13699, USA

² Department of Computer Engineering, Biruni University, Turkey

³ Department of Mathematics, Science Faculty, Firat University, Elazig, Turkey

⁴ Department of Medical Research, China Medical University Hospital, China Medical University, Taichung, Taiwan

⁵ Department of Basic Sciences and Related Studies, Mehran University of Engineering and Technology, Jamshoro – 76072, Sindh, Pakistan

⁶ Department of Mathematics, Near East University TRNC, Mersin 10, Turkey

⁷ Mathematics Research Center, Near East University TRNC, Mersin 10, Turkey

Received: 9 Mar. 2022, Revised: 21 Jun. 2022, Accepted: 5 Jul. 2022

Published online: 1 Jan. 2024

Abstract: During the current investigation, we examine the impact of a contagious disease on the growth of the ecological system. We study a non-integer-order predator-prey system by applying the Atangana-Baleanu-Caputo (ABC) derivative. Indeed, an effective numerical technique is exercised to discover the system's dynamic behavior using different values of the fractional-order parameter. Moreover, the existence of the results is given utilizing the fixed-point theorem. Also, diagrams via numerical simulations of the approximate solutions are explained in different dimensions. Finally, the analysis carried out in this manuscript helps us understand the several interactions among different species and protozoa that commonly occur in bio- and ecological systems.

Keywords: Mittag-Leffler kernel, fractional calculus, predator-prey system, fixed point analysis.

1 Introduction

The evolution of the qualitative investigation of ODEs is arising to analyze various enigmas in mathematical biology and related areas. Designing the model to the community dynamics of a prey-predator problem is an example of the significant and impressive aim in mathematical biology, that has undergone comprehensive reflection by many scholars [1, 2, 3, 4, 5, 6]. During real universe, several classes of prey and predator classes possess a living past which is formed of at least couple steps: immature and mature, and every step possesses various behavioral characteristics. Therefore, some activities of step-building prey-predator systems are presented in many articles in the literature [7, 8, 9, 10, 11, 12]. Contagious diseases occur if infected external bodies penetrate into the individual body.

The mentioned pathogens could be bacteria, microorganisms, and parasites. These bodies are transferred by virus from a different individual, creatures, polluted food, or disposal to any of the environmental constituents which are infected by any of the mentioned organisms. These diseases have several signs in body, containing raised one warmth and anxiety, moreover to additional traits which vary regarding the position of contamination, nature, and hardness of the infection. It is permissible to possess a disease that produces moderate signs, and hence it does not require to be solved.

* Corresponding author e-mail: evren.hincal@neu.edu.tr

Indeed, there are severe situations that may affect mortality. Also, they probably influence the population scale of several kinds. In a more dangerous situation, some species probably indeed become dead because of some fatal infections that occurred in some extremely rational populations. Mathematical systems for foretelling the progression of varieties of such pathogen have been utilized in an escalating way in the latest decades. The biological species are most susceptible to any disease that can affect the development of species. We study the predator-prey interplay. Such disease is able to influence the power of predators and performance of shooting, which places some predators at threat of extirpation. During the literature review, several investigations were examined on the predator-prey interplay in bearing the contagious infections [13,14,15,16,17].

On the other hand, there are various approaches that the predators examine for reaching prosperous hunting. Predator assistance is an efficient approach that several predators seek a unique prey. Such an approach can be so beneficial in degrading the hunting failure scale. Numerous anglers perform in the aforementioned approach. For instance, some animals such as lions, and dogs are distinguished for the great ability scale in this manner. Modelling of such particular performance of predator was firstly formed in [18] wherein an uncomplicated pattern was employed for representing such collaboration. There were studies that investigated such performance in the predator-prey interplay [19,20,21,22,23,24,25,26,27]. Regarding the achieved outcomes in [28], time-fractional derivative possesses wide applicability for explaining various real-life conditions, that is recognized with memory impact for the dynamical model; memory speed is named for non-integer order, memory function of kernel of non-integer derivative. The mentioned derivative (ABC) is applied to model several phenomena [29,30,31,32]. Regarding the mentioned inclinations, we examine the eco-epidemiological system given below:

$$\begin{aligned} \frac{du_1}{dt} &= f_1(u_1, u_2, u_3) = s_1(u_1(t) + u_2(t)) - (s_2 + s_3u_3(t))u_3(t)u_1(t) - s_4u_1(t)u_2(t) - s_5u_1(t), \\ \frac{du_2}{dt} &= f_2(u_1, u_2, u_3) = s_4u_1(t)u_2(t) - (s_2 + s_3u_3(t))u_3(t)u_2(t) - s_5u_2(t), \\ \frac{du_3}{dt} &= f_3(u_1, u_2, u_3) = s_6(s_2 + s_3u_3(t))u_3(t)(u_1(t) + u_2(t)) - s_7u_3(t), \end{aligned} \quad (1)$$

where it may be noted that the state variables $u_1(t)$, $u_2(t)$, and $u_3(t)$ respectively stand for densities of susceptible prey, infected prey, and the predator populations. Regarding initial conditions (ICs), we have $u_1(0) = u_{1,0}(t)$, $u_2(0) = u_{2,0}(t)$ and $u_3(0) = u_{3,0}(t)$. Moreover, one can see that there are 7 parameters playing the vital role for the dynamics of the model's behavior. Description of these parameters is detailed in the Table 1.

Table 1: Small Vital parameters involved in the eco-epidemiological system.

Parameters	Description
s_1	Reproduction number of the prey population
$(s_2 + s_3u_3(t))u_3(t)u_1(t)$ & $(s_2 + s_3u_3(t))u_3(t)u_2(t)$	Hunting cooperation functional [18]
s_4	Transmission rate of the prey population (infection rate)
s_5	Death rate of the prey population
s_6	Conversion rate of prey biomass into predator biomass
s_7	Natural mortality of the predator population

The next section is selected to implement some fundamental definitions to comprehend remaining analysis carried out in other forthcoming sections.

2 Essential Definitions

Definition 1. Riemann–Liouville derivative of order $\alpha > 0$ for function X is defined as

$${}^{RL}\mathcal{D}_t^\alpha X(t) = \frac{1}{\Gamma(n-\alpha)} \int_0^t \frac{X^{(n)}(\zeta)}{(t-\zeta)^{n-\alpha+1}} d\zeta, \quad n-1 < \alpha < n. \quad (2)$$

Definition 2. Caputo derivative of order $\alpha > 0$ of $X : (0, \infty) \rightarrow \mathbf{R}$ is defined as

$${}^C \mathcal{D}_t^\alpha X(t) = \frac{1}{\Gamma(n - \alpha)} \int_0^t (t - \zeta)^{n - \alpha - 1} X^{(n)}(\zeta) d\zeta, \tag{3}$$

where $\lceil \cdot \rceil$ signifies the ceiling function and $n = \lceil \alpha \rceil$, and $0 < \alpha \leq 1$.

Definition 3. Suppose $X \in H^1(a, b)$, $b > a$, $\alpha \in [0, 1]$ so, the Caputo–Fabrizio derivative is:

$${}^{CF} \mathcal{D}_t^\alpha (X(t)) = \frac{W(\alpha)}{1 - \alpha} \int_a^t X'(\zeta) \exp \left[-\alpha \frac{t - \zeta}{1 - \alpha} \right] d\zeta, \tag{4}$$

where $W(\alpha)$ for $W(0) = W(1)$ expresses a normalization function and exerting $X \notin H^1(a, b)$ we own

$${}^{CF} \mathcal{D}_t^\alpha (X(t)) = \frac{\alpha W(\alpha)}{1 - \alpha} \int_a^t (X(t) - X(\zeta)) \exp \left[-\alpha \frac{t - \zeta}{1 - \alpha} \right] d\zeta, \tag{5}$$

Definition 4. Consider $X \in H^1(a, b)$, $a < b$ and $\alpha \in [0, 1]$ so the Atangana–Baleanu derivative for X in the Caputo structure is written as

$${}^{ABC} \mathcal{D}_t^\alpha X(t) = \frac{W(\alpha)}{1 - \alpha} \int_a^t X'(y) E_\alpha \left[-\alpha \frac{(t - \zeta)^\alpha}{1 - \alpha} \right] d\zeta, \tag{6}$$

where E_α is known as the Mittag–Leffler function explained in [33, 34].

$$E_\alpha(z) = \sum_{n=0}^{\infty} \frac{z^n}{\Gamma(n\alpha + 1)},$$

Theorem 1. Consider the differential equation containing the Atangana–Baleanu differential operator:

$${}^{ABC} \mathcal{D}_t^\alpha f(t) = u(t). \tag{7}$$

The foregoing equation possesses a unique answer if the subsequent theorem is performed

$$f(t) = \frac{1 - \alpha}{W(\alpha)} u(t) + \frac{\alpha}{W(\alpha)\Gamma(p)} \int_0^t u(\zeta)(t - \zeta)^{\alpha - 1} d\zeta,$$

To view the evidence of the stated theorem, we refer to [35]. The common time-fractional order of the differential equation described in (7) is a problem of the form

$$\mathcal{D}^\alpha X(t) = F(X(t), t), \alpha \in (0, 1), \tag{8}$$

Theorem 2. Suppose a function $Q(X(t))$ exists, that results in a negative semi-definite non-integer function defined $\mathcal{D}^p Q(X(t))$ by $p \in (0, 1]$, so the model (2) would be stable, periodically and [36, 37] is given to depict the analysis of stability.

3 Analysis by Non-integer Order

We suppose $\mathfrak{B} = \mathcal{B}(L) \times \mathcal{B}(L)$, which $\mathcal{B}(L)$ named continuous Branch function on interval L containing

$$\|u_1, u_2, u_3\| = \|u_1\| + \|u_2\| + \|u_3\|,$$

which $\|u_1\| = \sup \{ |u_1(t)| : t \in L \}$, $\|u_2\| = \sup \{ |u_2(t)| : t \in L \}$ and $\|u_3\| = \sup \{ |u_3(t)| : t \in L \}$, Following, we develop the problem (1) by interchanging the traditional derivative by ABC one:

$$\begin{aligned} {}^{ABC} \mathcal{D}_t^\alpha u_1(t) &= s_1(u_1(t) + u_2(t)) - (s_2 + s_3 u_3)u_3(t)u_1(t) - s_4 u_1(t)u_2(t) - s_5 u_1(t), \\ {}^{ABC} \mathcal{D}_t^\alpha u_2(t) &= s_4 u_1(t)u_2(t) - (s_2 + s_3 u_3)u_3(t)u_2(t), \\ {}^{ABC} \mathcal{D}_t^\alpha u_3(t) &= s_5(s_2 + s_3 u_3(t))u_3(t)(u_1(t) + u_2(t)) - s_5, \end{aligned} \tag{9}$$

Regarding ICs

$$u_1(0) = u_{1,0}(t), u_2(0) = u_{2,0}(t), u_3(0) = u_{3,0}(t), \quad (10)$$

Under adopting the notion of the Atangana-Baleanu-Caputo derivative and the Theory of [Theorem 1](#), we reconstruct (2) to fractional Volterra integral of problem formation

$$\begin{aligned} u_1(t) - u_1(0) &= \frac{1-\alpha}{W(\alpha)} [s_1(u_1(t) + u_2(t)) - (s_2 + s_3u_3)u_3(t)u_1(t) - s_4u_1(t)u_2(t) - s_5u_1(t)] \\ &+ \frac{\alpha}{W(\alpha)\Gamma(\alpha)} \int_0^t (t-\zeta)^{\alpha-1} \times [s_1(u_1(t) + u_2(t)) - (s_2 + s_3u_3)u_3(t)u_1(t) - s_4u_1(t)u_2(t) - s_5u_1(t)] d\zeta, \\ u_2(t) - u_2(0) &= \frac{1-\alpha}{W(\alpha)} [s_4u_1(t)u_2(t) - (s_2 + s_3u_3)u_3(t)u_2(t)] \\ &+ \frac{\alpha}{W(\alpha)\Gamma(\alpha)} \int_0^t (t-\zeta)^{\alpha-1} \times [s_4u_1(t)u_2(t) - (s_2 + s_3u_3)u_3(t)u_2(t)] d\zeta, \\ u_3(t) - u_3(0) &= \frac{1-\alpha}{W(\alpha)} [s_5(s_2 + s_3u_3(t))u_3(t)(u_1(t) + u_2(t)) - s_5] \\ &+ \frac{\alpha}{W(\alpha)\Gamma(\alpha)} \int_0^t (t-\zeta)^{\alpha-1} \times [s_6(s_2 + s_3u_3(t))u_3(t)(u_1(t) + u_2(t)) - s_7u_3(t)] d\zeta, \end{aligned} \quad (11)$$

Now, we take

$$\begin{aligned} \mathcal{B}_1(u_1, t) &= s_1(u_1(t) + u_2(t)) - (s_2 + s_3u_3)u_3(t)u_1(t) - s_4u_1(t)u_2(t) - s_5u_1(t) \\ \mathcal{B}_2(u_2, t) &= [s_4u_1(t)u_2(t) - (s_2 + s_3u_3)u_3(t)u_2(t)] \\ \mathcal{B}_3(u_3, t) &= s_6(s_2 + s_3u_3(t))u_3(t)(u_1(t) + u_2(t)) - s_7u_3(t) \end{aligned} \quad (12)$$

Beside, we provide the subsequent result.

Lemma 1. The kernels $\mathcal{B}_i(S, t)$, for $i = 1, 2, 3$ hold the Lipschitz condition for $0 \leq \mathcal{B}_i(u_i, t) < 1, i = 1, 2, 3$.

Proof. Opening by $i = 1$ we own $\mathcal{B}_1(u_1, t) = r(u_1(t) + u_2(t)) - (\lambda + au_3)u_3(t)u_1(t) - \delta_1(t)u_2(t) - \mu u_1(t)$. Let u_1 and u_1^* , then we own

$$\|\mathcal{B}_1(u_1, t) - \mathcal{B}_1(u_1^*, t)\| = \|\alpha \{u_1(t) - u_1^*(t)\}\| \leq \|\alpha\| \|u_1(t) - u_1^*(t)\| \leq G_1 \|u_1(t) - u_1^*(t)\| \quad (13)$$

which $G_1 = \alpha$. Take $m_1 = \max_{t \in L} \|u_1(t)\|$, $m_2 = \max_{t \in L} \|u_2(t)\|$ and $m_3 = \max_{t \in L} \|u_3(t)\|$ be limited functions, so

$$\|\mathcal{B}_1(u_1, t) - \mathcal{B}_1(u_1^*, t)\| \leq G_1 \|u_1(t), u_1^*(t)\|$$

resembling phrases for components x_i , for $i = 2, 3$ to get $\|\mathcal{B}_i(u_i, t) - \mathcal{B}_i(u_i^*, t)\| \leq G_i \|u_i(t), u_i^*(t)\|$, for $i = 2, 3$. Hence, the Lipschitz condition works for \mathcal{B}_1 , and contraction works for $0 \leq G_1 < 1$. Using the considered kernels (11) results

$$\begin{aligned} u_1(t) &= u_1(0) + \frac{1-\alpha}{W(\alpha)} \mathcal{B}_1(u_1, t) + \frac{\alpha}{W(\alpha)\Gamma(\alpha)} \int_0^t (t-\zeta)^{\alpha-1} \mathcal{B}_1(\zeta, u_1) d\zeta, \\ u_2(t) &= u_2(0) + \frac{1-\alpha}{W(\alpha)} \mathcal{B}_2(u_2, t) + \frac{\alpha}{W(\alpha)\Gamma(\alpha)} \int_0^t (t-\zeta)^{\alpha-1} \mathcal{B}_2(\zeta, u_2) d\zeta, \\ u_3(t) &= u_3(0) + \frac{1-\alpha}{W(\alpha)} \mathcal{B}_3(u_3, t) + \frac{\alpha}{W(\alpha)\Gamma(\alpha)} \int_0^t (t-\zeta)^{\alpha-1} \mathcal{B}_3(\zeta, u_3) d\zeta, \end{aligned} \quad (14)$$

by similar recursive equations

$$\begin{aligned} u_{1,n}(t) &= \frac{1-\alpha}{W(\alpha)} \mathcal{B}_1(u_{1,n-1}, t) + \frac{\alpha}{W(\alpha)\Gamma(\alpha)} \int_0^t (t-\zeta)^{\alpha-1} \mathcal{B}_1(\zeta, u_{1,n-1}) d\zeta, \\ u_{2,n}(t) &= \frac{1-\alpha}{W(\alpha)} \mathcal{B}_2(u_{2,n-1}, t) + \frac{\alpha}{W(\alpha)\Gamma(\alpha)} \int_0^t (t-\zeta)^{\alpha-1} \mathcal{B}_2(\zeta, u_{2,n-1}) d\zeta, \\ u_{3,n}(t) &= \frac{1-\alpha}{W(\alpha)} \mathcal{B}_3(u_{3,n-1}, t) + \frac{\alpha}{W(\alpha)\Gamma(\alpha)} \int_0^t (t-\zeta)^{\alpha-1} \mathcal{B}_3(\zeta, u_{3,n-1}) d\zeta, \end{aligned} \quad (15)$$

The difference among consecutive terms in the denoting is offering with

$$\begin{aligned}
 Z1_n(t) &\equiv u_{1,n}(t) - u_{1,n-1}(t) = \frac{1-\alpha}{W(\alpha)} [\mathcal{B}_1(u_{1,n-1},t) - \mathcal{B}_1(u_{1,n-2},t)] \\
 &\quad + \frac{\alpha}{W(\alpha)\Gamma(\alpha)} \int_0^t (t-\zeta)^{\alpha-1} [\mathcal{B}_1(\zeta, u_{1,n-1}) - \mathcal{B}_1(\zeta, u_{1,n-2})] d\zeta, \\
 Z2_n(t) &\equiv u_{2,n}(t) - u_{2,n-1}(t) = \frac{1-\alpha}{W(\alpha)} [\mathcal{B}_2(u_{2,n-1},t) - \mathcal{B}_2(u_{2,n-2},t)] \\
 &\quad + \frac{\alpha}{W(\alpha)\Gamma(\alpha)} \int_0^t (t-\zeta)^{\alpha-1} [\mathcal{B}_2(\zeta, u_{2,n-1}) - \mathcal{B}_2(\zeta, u_{2,n-2})] d\zeta, \\
 Z3_n(t) &\equiv u_{3,n}(t) - u_{3,n-1}(t) = \frac{1-\alpha}{W(\alpha)} [\mathcal{B}_3(u_{3,n-1},t) - \mathcal{B}_3(u_{3,n-2},t)] \\
 &\quad + \frac{\alpha}{W(\alpha)\Gamma(\alpha)} \int_0^t (t-\zeta)^{\alpha-1} [\mathcal{B}_3(\zeta, u_{3,n-1}) - \mathcal{B}_3(\zeta, u_{3,n-2})] d\zeta,
 \end{aligned} \tag{16}$$

we state that

$$u_{i,n} = \sum_{j=1}^n Zi_j(t), i = 1, 2, 3.$$

Now, we take (16) and use the norm to have

$$\begin{aligned}
 \|Z1_n\| = \|u_{1,n}(t) - u_{1,n-1}(t)\| &\leq \frac{1-\alpha}{W(\alpha)} \|\mathcal{B}_1(u_{1,n-1},t) - \mathcal{B}_1(u_{1,n-2},t)\| + \frac{p}{W(\alpha)\Gamma(\alpha)} \\
 &\quad \times \left\| \int_0^t (t-\zeta)^{\alpha-1} [\mathcal{B}_1(u_{1,n-1},t) - \mathcal{B}_1(u_{1,n-2},t)] d\zeta \right\|.
 \end{aligned} \tag{17}$$

To satisfy the Lipschitz condition, we have

$$\begin{aligned}
 \|u_{1,n}(t) - u_{1,n-1}(t)\| &\leq \frac{1-\alpha}{W(\alpha)} \chi_1 \|u_{1,n-1} - u_{1,n-2}\| \\
 &\quad + \frac{p}{W(\alpha)\Gamma(\alpha)} \times \chi_1 \int_0^t (t-\zeta)^{\alpha-1} \|u_{1,n-1} - u_{1,n-2}\| d\zeta,
 \end{aligned} \tag{18}$$

and

$$\|Z1_n\| \leq \frac{1-\alpha}{W(\alpha)} \chi_1 \|Z1_{n-1}\| + \frac{\alpha}{W(\alpha)\Gamma(\alpha)} \times \chi_1 \int_0^t (t-\zeta)^{\alpha-1} \|Z1_{n-1}(\zeta)\| d\zeta, \tag{19}$$

Equivalent expressions guard for rest elements:

$$\|Zi_n\| \leq \frac{1-\alpha}{W(\alpha)} \chi_1 \|Zi_{n-1}\| + \frac{\alpha}{W(\alpha)\Gamma(\alpha)} \times \chi_1 \int_0^t (t-\zeta)^{\alpha-1} \|Zi_{n-1}(\zeta)\| d\zeta, \quad i = 2, 3, \tag{20}$$

We take solutions $X_1(t), X_2(t)$ and $X_3(t)$ exist for model (9) that indicates

$$\begin{aligned}
 \|u_1(t) - X_1(t)\| &\leq \frac{1-\alpha}{W(\alpha)} [\mathcal{B}_1(u_1,t) - \mathcal{B}_1(X_1,t)] \\
 &\quad + \frac{\alpha}{W(\alpha)\Gamma(\alpha)} \int_0^t (t-\zeta)^{\alpha-1} [\mathcal{B}_1(u_1,t) - \mathcal{B}_1(X_1,t)] d\zeta \\
 &\leq \frac{1-\alpha}{W(\alpha)} \|\mathcal{B}_1(u_1,t) - \mathcal{B}_1(X_1,t)\| \\
 &\quad + \frac{\alpha}{W(\alpha)\Gamma(\alpha)} \int_0^t (t-\zeta)^{\alpha-1} \|\mathcal{B}_1(u_1,t) - \mathcal{B}_1(X_1,t)\| d\zeta,
 \end{aligned} \tag{21}$$

By regarding traits of the Lipschitz condition yields in

$$\|u_1(t) - X_1(t)\| \leq \frac{1-\alpha}{W(\alpha)} \chi_1 \|u_1(t) - X_1(t)\| + \frac{\chi_1 t^\alpha}{W(\alpha)\Gamma(\alpha)} \|u_1(t) - X_1(t)\| \tag{22}$$

which results

$$\|u_1(t) - X_1(t)\| \left[1 - \frac{\chi_1(1-\alpha)}{W(\alpha)} + \frac{\chi_1 t^\alpha}{W(\alpha)\Gamma(\alpha)} \right] \leq 0 \quad (23)$$

with $\|u_1(t) - X_1(t)\| = 0$, it indicates $u_1(t) = X_1(t)$. Alike phrases exist for segments $u_i(t), i = 2, 3$. Consequently, the fractional problem (9) owns a unique answer.

3.1 Numerical Scheme

Now, we practice the numerical approach developed in [38] to resolve the problem for simulations. The method has the following form:

$$u_{n+1} = u_0 + \frac{1-\alpha}{W(\alpha)} f(u(t_n), t_n) + \frac{\alpha}{W(\alpha)} \sum_{q=0}^n \left\{ \frac{h^\alpha f(u_q, t_q)}{\Gamma(\alpha+2)} a_n - \frac{h^\alpha f(u_{q-1}, t_{q-1})}{\Gamma(\alpha+2)} b_n \right\} + E_n^\alpha, \quad (24)$$

where $a_n = (n+1-q)^\alpha(n-q+2+\alpha) - (n-q)^\alpha(n-q+2+2\alpha)$ and $b_n = (n+1-q)^{\alpha+1} - (n-1)^\alpha(n-q+1+\alpha)$ and the remaining term E_n^α is expressed by

$$E_n^\alpha = \frac{\alpha}{W(\alpha)\Gamma(\alpha)} \sum_{q=0}^n \int_{t_q}^{t_{q-1}} \frac{(\zeta - t_q)(\zeta - t_{q-1})}{2} \frac{\partial^2}{\partial \zeta^2} \times [f(u(\zeta), \zeta)]_{\zeta=\lambda_\zeta} (t_{n+1} - \zeta)^{\alpha-1} d\zeta, \quad (25)$$

To understand more of this approach, we recommend the work carried out in [38]. So, exercising the kernels, Eq.(14) changes to the following

$$\begin{aligned} u_1(t) &= u_1(0) + \frac{1-\alpha}{W(\alpha)} \mathcal{B}_1(u_1(t), t) + \frac{\alpha}{W(\alpha)\Gamma(\alpha)} \int_0^t (t-\zeta)^{\alpha-1} \mathcal{B}_1(\zeta, u_1(\zeta)) d\zeta, \\ u_2(t) &= u_2(0) + \frac{1-\alpha}{W(\alpha)} \mathcal{B}_2(u_2(t), t) + \frac{\alpha}{W(\alpha)\Gamma(\alpha)} \int_0^t (t-\zeta)^{\alpha-1} \mathcal{B}_2(\zeta, u_2(\zeta)) d\zeta, \\ u_3(t) &= u_3(0) + \frac{1-\alpha}{W(\alpha)} \mathcal{B}_3(u_3(t), t) + \frac{\alpha}{W(\alpha)\Gamma(\alpha)} \int_0^t (t-\zeta)^{\alpha-1} \mathcal{B}_3(\zeta, u_3(\zeta)) d\zeta. \end{aligned} \quad (26)$$

Thus, exercising the technique given in (24) at $t = t_{n+1}$, we own

$$\begin{aligned} u_{1,n+1} &= u_{1,0} + \frac{1-\alpha}{W(\alpha)} \mathcal{B}_1(u_1(t_n), t_n) + \frac{\alpha}{W(\alpha)} \sum_{q=0}^n \left\{ \frac{h^\alpha \mathcal{B}_1(u_{1,q}, t_q)}{\Gamma(\alpha+2)} a_n - \frac{h^\alpha \mathcal{B}_1(u_{1,q-1}, t_{q-1})}{\Gamma(\alpha+2)} b_n \right\} + {}^1 E_n^\alpha, \\ u_{2,n+1} &= u_{2,0} + \frac{1-\alpha}{W(\alpha)} \mathcal{B}_2(u_2(t_n), t_n) + \frac{\alpha}{W(\alpha)} \sum_{q=0}^n \left\{ \frac{h^\alpha \mathcal{B}_2(u_{2,q}, t_q)}{\Gamma(\alpha+2)} a_n - \frac{h^p \mathcal{B}_2(u_{2,s-1}, t_{s-1})}{\Gamma(p+2)} b_n \right\} + {}^2 E_n^\alpha, \\ u_{3,n+1} &= u_{3,0} + \frac{1-\alpha}{W(\alpha)} \mathcal{B}_3(u_3(t_n), t_n) + \frac{\alpha}{W(\alpha)} \sum_{q=0}^n \left\{ \frac{h^\alpha \mathcal{B}_3(u_{3,q}, t_q)}{\Gamma(\alpha+2)} a_n - \frac{h^p \mathcal{B}_3(u_{3,q-1}, t_{q-1})}{\Gamma(\alpha+2)} b_n \right\} + {}^3 E_n^\alpha, \end{aligned} \quad (27)$$

by $a_n = (n+1-q)^\alpha(n-q+2+\alpha) - (n-q)^\alpha(n-q+2+2\alpha)$, $b_n = (n+1-q)^{\alpha+1} - (n-q)^\alpha(n-q+1+\alpha)$ and ${}^i E_n^\alpha$ for $i = 1, 2, 3$ is depicted as

$${}^i E_n^\alpha = \frac{\alpha}{W(\alpha)\Gamma(p)} \sum_{q=0}^n \int_{t_q}^{t_{q-1}} \frac{(\zeta - t_q)(\zeta - t_{q-1})}{2} \frac{\partial^2}{\partial \zeta^2} [\mathcal{B}_i(u(\zeta), \zeta)]_{\zeta=\lambda_\zeta} (t_{n+1} - \zeta)^{\alpha-1} d\zeta, \quad (28)$$

The following section is dedicated to reveal the performance of the above discussed numerical scheme.

4 Numerical Experiments

Now, we use the proposed numerical scheme as discussed in the above-mentioned section to get the approximate solutions of the eco-epidemiological system as suggested in the present study under the novel fractional operator with the name of ABC. We solve the system for different values of fractional order α . Figures 1 to 3 show the results for different values of α and also for different values of the ICs including $u_1(0) = 0.01, u_2(0) = 1.1$ and $u_3(0) = 0.05$ for $s_1 = 1.5, s_2 = 1.5, s_3 = 0.5, s_4 = 0.5, s_5 = 0.5, s_6 = 0.5$ and $s_7 = 0.5$. The fractional orders taken for these figures are 0.95, 0.96, 0.97 and 0.98. Indeed, the figures 4 to 6 are dedicated to depict the results for α values and with ICs given as $u_1(0) = 0.01, u_2(0) = 1.1$ and $u_3(0) = 0.05$ for $s_1 = 1.5, s_2 = 0.5, s_3 = 0.5, s_4 = 0.5, s_5 = 0.5, s_6 = 0.5$ and $s_7 = 0.5$; successfully. Similarly, figures 7 to 27 are obtained to show the results for $s_1, s_2, s_3, s_4, s_5, s_6$ and s_7 along with the selected fractional orders for the parameter $\alpha > 0$.

In the Figure 1, each state variable is simulated over considerably large time interval $[0, 500]$ to understand dynamics of their behaviour. It is observed that the densities of susceptible prey, and predator populations highly fluctuate under selected ICs and the parameters whereas the density of the infected prey sharply decrease over a very small time interval and then goes to vanish as quickly as possible and this situation occurs because susceptible and the predator population are at greater variation.

If we closely look at the Figure 2 then we realize that that patterns like limit cycles occur in the phase portrait forms under different values of α and the parameters. Some strange chaotic type behavior is observed in the figure which is not possible to obtain with classical version of the eco-epidemiological system, that is, when $\alpha = 1$. Similarly, Figure 3 shows 3-dimensional plot for the underlying system wherein, once again, chaotic type behavior with predator-prey limit cycles is observed. This phenomenon is highly obvious in natural situations as well. Thus, it is said that ABC operator is capable enough to capture the most natural occurrences in the world.

The Figure 4 is obtained with a slight variation in the s_2 parameter that appears in the hunting cooperation functional as described in the Table 1. By decreasing s_2 from 1.5 to 0.5 in the figure 4, it is observed that the peaks of the fluctuations within the susceptible prey and predator populations decrease including the peak in the infected prey. However, there are still limit cycles having varying structures are observed as can be seen in the Figures 5 (2D phase-plane diagrams) and 6 (3 dimensional dynamics). While keeping the ICs same and varying some values of the parameters, we observe drastic change in the dynamics of the eco-epidemiological system as can be seen in the time series plots in the Figure 7 wherein one can note that the not only peak of fluctuations decrease but the infected prey slightly increase also. One may also note that as value of fractional order α approaches 1, the fluctuations increase. Some interesting limit cycles in the form of phase-planes and 3 dimensional plots are also depicted in the Figures 8 and 9; respectively.

Looking at the Figure 10, one can observe that there comes huge change in the behavior of all three populations when parameters are varied particularly the parameters s_3 and s_7 with little bit high values while ICs and the fractional order α are still same as considered in previous figures. Limit cycles as shown in the Figure 11 are reduced in size and this happens due to the fact that now there are not many fluctuations in the populations. Similarly, the Figure 12 refers the chaotic behavior that lasts for smaller interval of time.

Likewise, upon carrying out numerous other simulations of the eco-epidemiological system as suggested in the present study under the novel fractional operator with the name of ABC, we have obtained interesting dynamics and patterns that were not not encountered with operators having no memory such as those classical ones also called integer-order derivatives. These other simulations based upon time series, phase-portraits and 3 dimensional structures can be visualized in the Figures from 13 to 27 wherein different parameters' values are taken into consideration in order to obtain the various kinds of behavior for the system via ABC operator.

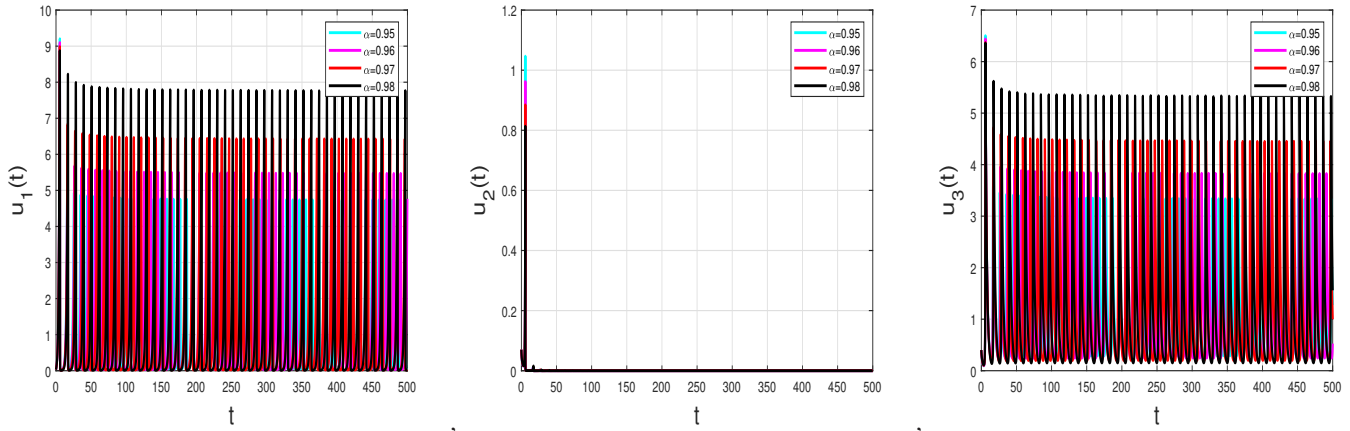


Fig. 1: Plot of solutions for different values of α with ICs $u_1(0) = 0.01, u_2(0) = 1.1$ and $u_3(0) = 0.05$ for parameters $s_1 = 1.5, s_2 = 1.5, s_3 = 0.5, s_4 = 0.5, s_5 = 0.5, s_6 = 0.5$ and $s_7 = 0.5$.

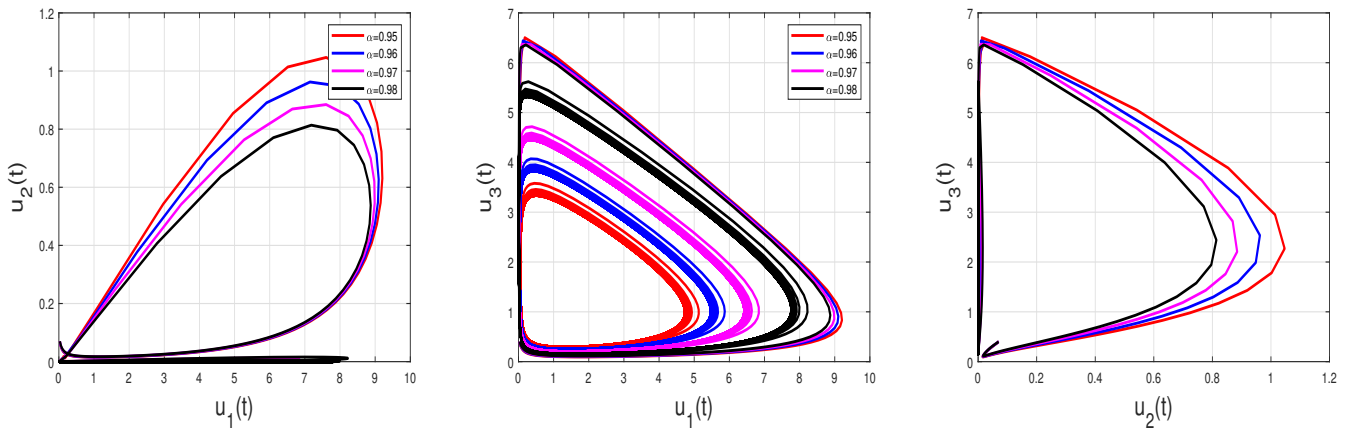


Fig. 2: 2D plots of solutions for different values of α with ICs $u_1(0) = 0.01, u_2(0) = 1.1$ and $u_3(0) = 0.05$ for $s_1 = 1.5, s_2 = 1.5, s_3 = 0.5, s_4 = 0.5, s_5 = 0.5, s_6 = 0.5$ and $s_7 = 0.5$.

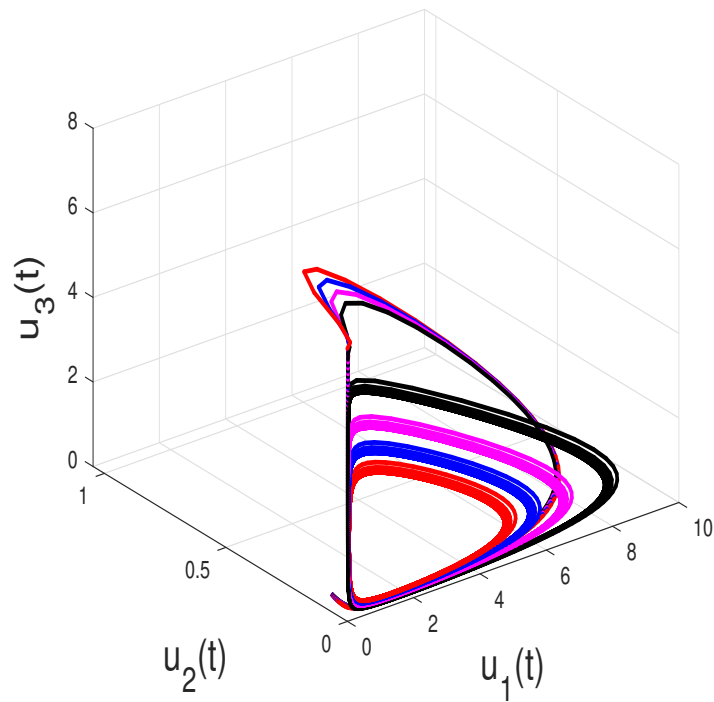


Fig. 3: Chaotic behaviour of of solutions for different values of α with ICs $u_1(0) = 0.01, u_2(0) = 1.1$ and $u_3(0) = 0.05$ for $s_1 = 1.5, s_2 = 1.5, s_3 = 0.5, s_4 = 0.5, s_5 = 0.5, s_6 = 0.5$ and $s_7 = 0.5$.

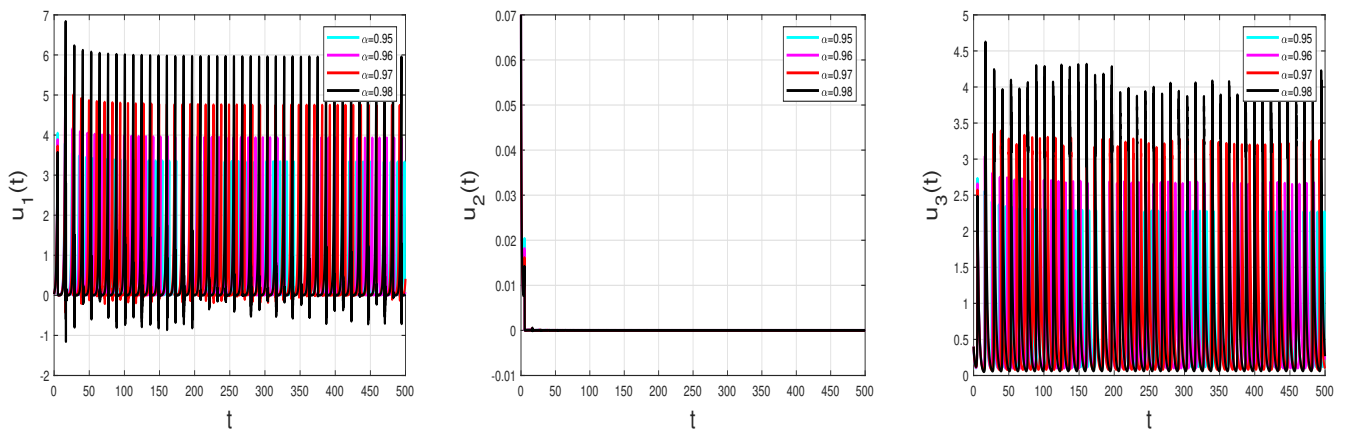


Fig. 4: Plot of solutions for different values of α with ICs $u_1(0) = 0.01, u_2(0) = 1.1$ and $u_3(0) = 0.05$ for $s_1 = 1.5, s_2 = 0.5, s_3 = 0.5, s_4 = 0.5, s_5 = 0.5, s_6 = 0.5$ and $s_7 = 0.5$.

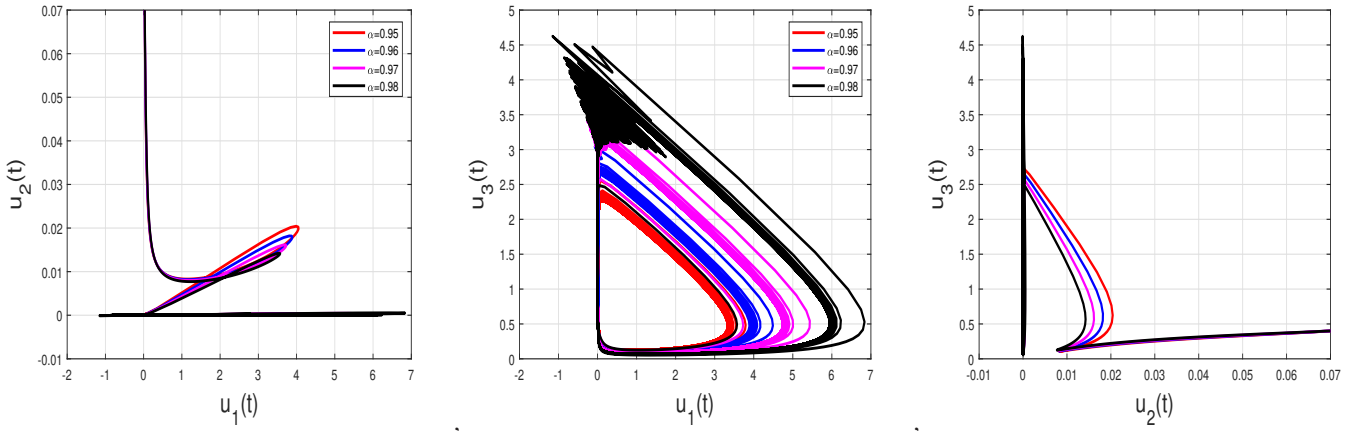


Fig. 5: 2D plot of solutions for different values of α with ICs $u_1(0) = 0.01, u_2(0) = 1.1$ and $u_3(0) = 0.05$ for $s_1 = 1.5, s_2 = 0.5, s_3 = 0.5, s_4 = 0.5, s_5 = 0.5, s_6 = 0.5$ and $s_7 = 0.5$.

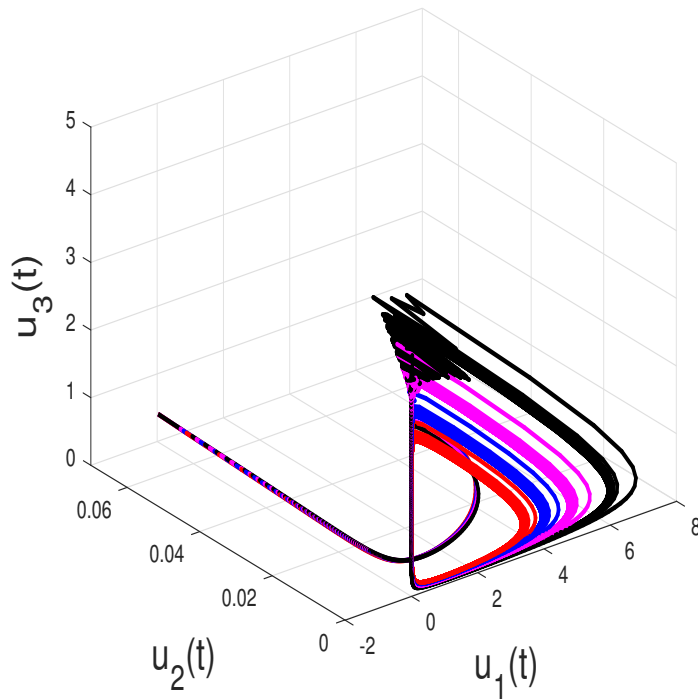


Fig. 6: 2D plot of solutions for different values of α with ICs $u_1(0) = 0.01, u_2(0) = 1.1$ and $u_3(0) = 0.05$ for $s_1 = 1.5, s_2 = 0.5, s_3 = 0.5, s_4 = 0.5, s_5 = 0.5, s_6 = 0.5$ and $s_7 = 0.5$.

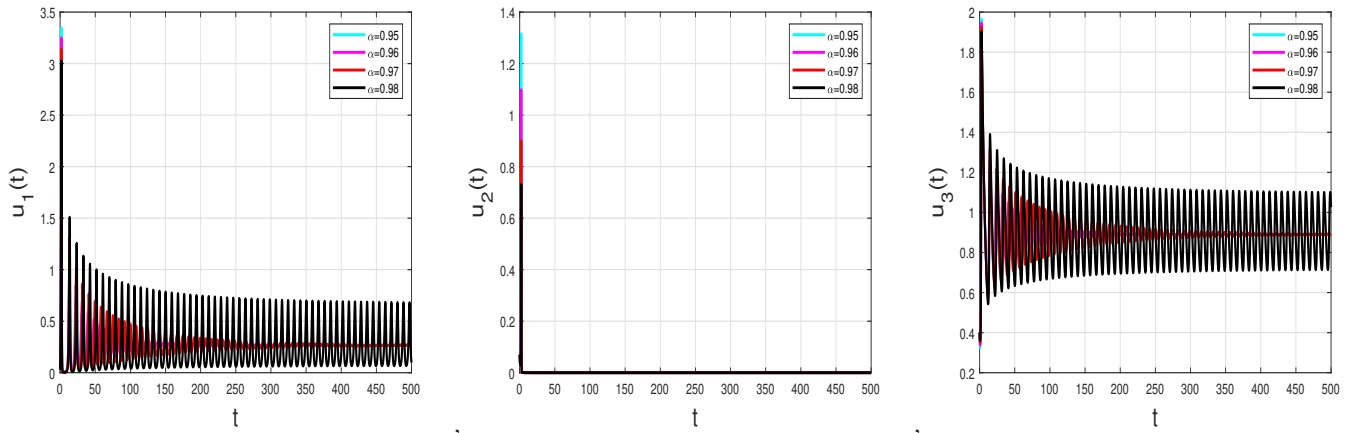


Fig. 7: Plot of solutions for different values of α with ICs $u_1(0) = 0.01, u_2(0) = 1.1$ and $u_3(0) = 0.05$ for $s_1 = 3.5, s_2 = 3.05, s_3 = 0.8, s_4 = 2.5, s_5 = 0.15, s_6 = 0.5$ and $s_7 = 0.3$.

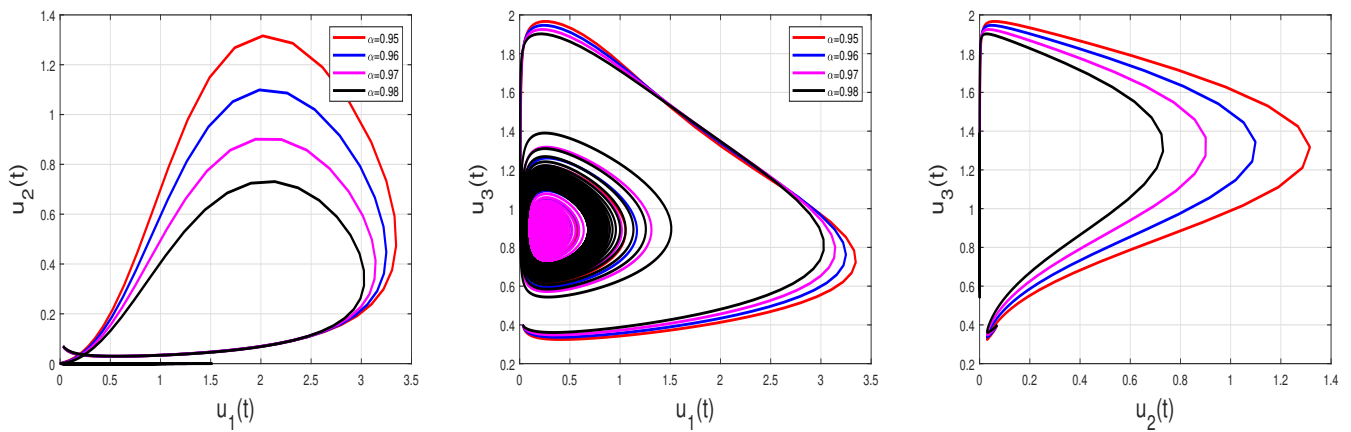


Fig. 8: 2D plot of solutions for different values of α with ICs $u_1(0) = 0.01, u_2(0) = 1.1$ and $u_3(0) = 0.05$ for $s_1 = 3.5, s_2 = 3.05, s_3 = 0.8, s_4 = 2.5, s_5 = 0.15, s_6 = 0.5$ and $s_7 = 0.3$.

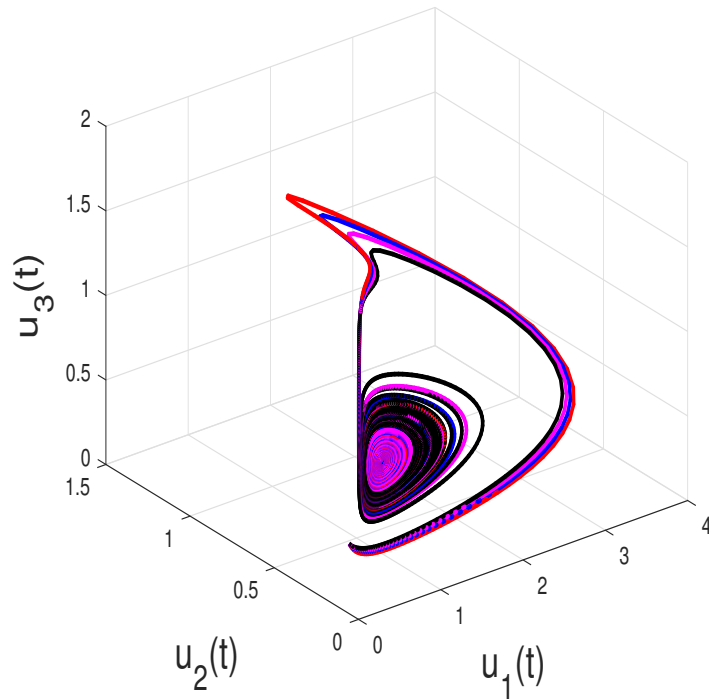


Fig. 9: Chaotic behaviour of of solutions for different values of α with ICs $u_1(0) = 0.01, u_2(0) = 1.1$ and $u_3(0) = 0.05$ for $s_1 = 3.5, s_2 = 3.05, s_3 = 0.8, s_4 = 2.5, s_5 = 0.15, s_6 = 0.5$ and $s_7 = 0.3$.

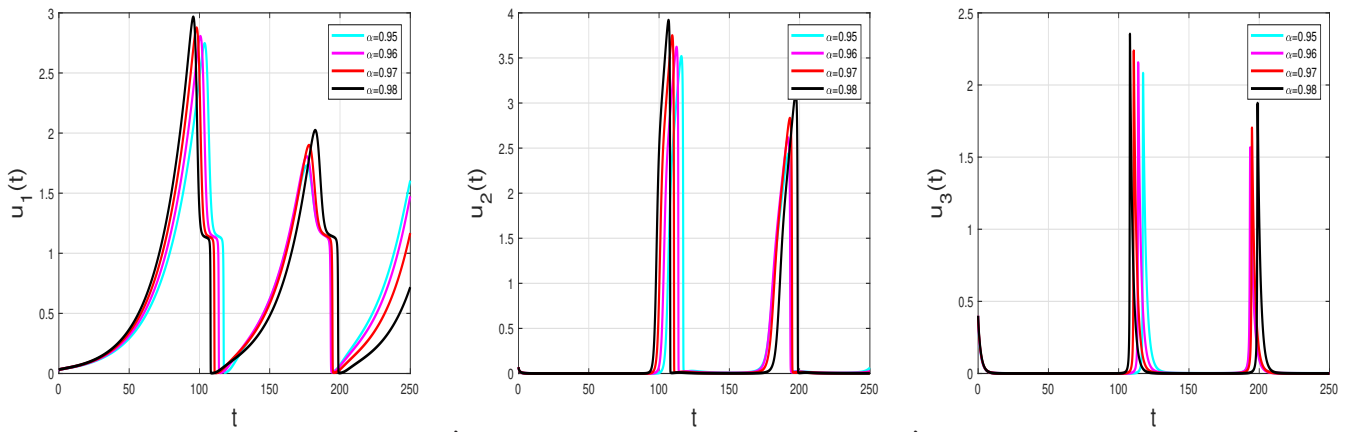


Fig. 10: Plot of solutions for different values of α with ICs $u_1(0) = 0.01, u_2(0) = 1.1$ and $u_3(0) = 0.05$ for $s_1 = 0.55, s_2 = 0.5, s_3 = 3.5, s_4 = 0.5, s_5 = 0.5, s_6 = 0.5$ and $s_7 = 1.5$.

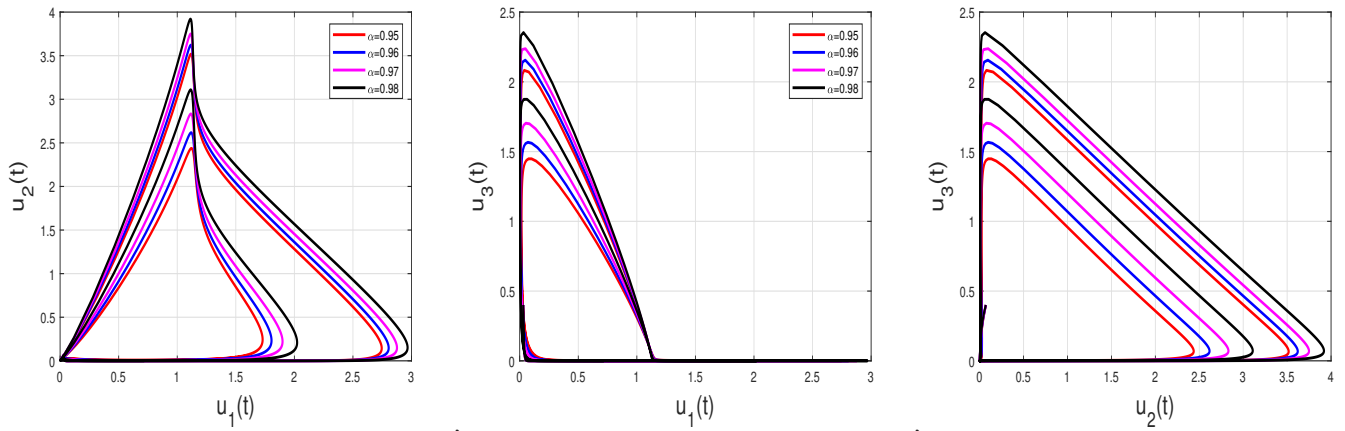


Fig. 11: 2D plot of solutions for different values of α with ICs $u_1(0) = 0.01, u_2(0) = 1.1$ and $u_3(0) = 0.05$ for $s_1 = 0.55, s_2 = 0.5, s_3 = 3.5, s_4 = 0.5, s_5 = 0.5, s_6 = 0.5$ and $s_7 = 1.5$.

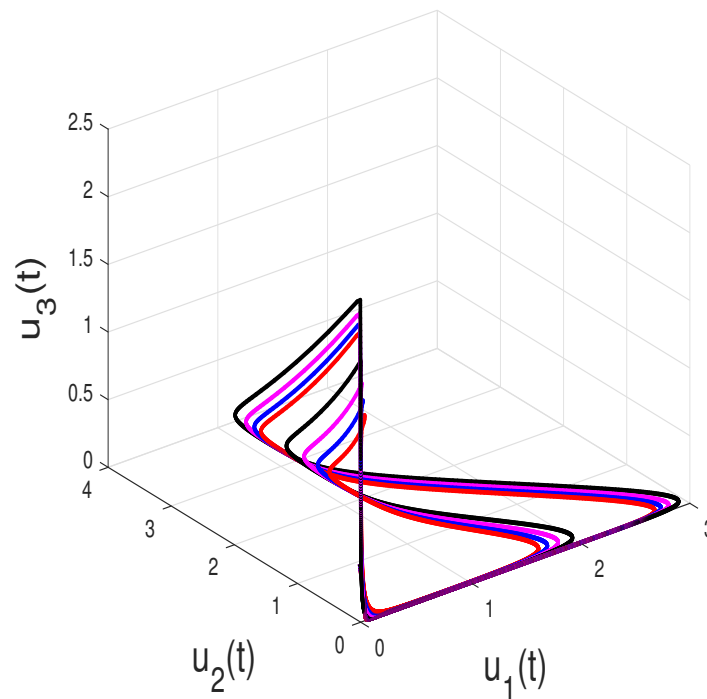


Fig. 12: Chaotic behaviour of of solutions for different values of α with ICs $u_1(0) = 0.01, u_2(0) = 1.1$ and $u_3(0) = 0.05$ for $s_1 = 0.55, s_2 = 0.5, s_3 = 3.5, s_4 = 0.5, s_5 = 0.5, s_6 = 0.5$ and $s_7 = 1.5$.

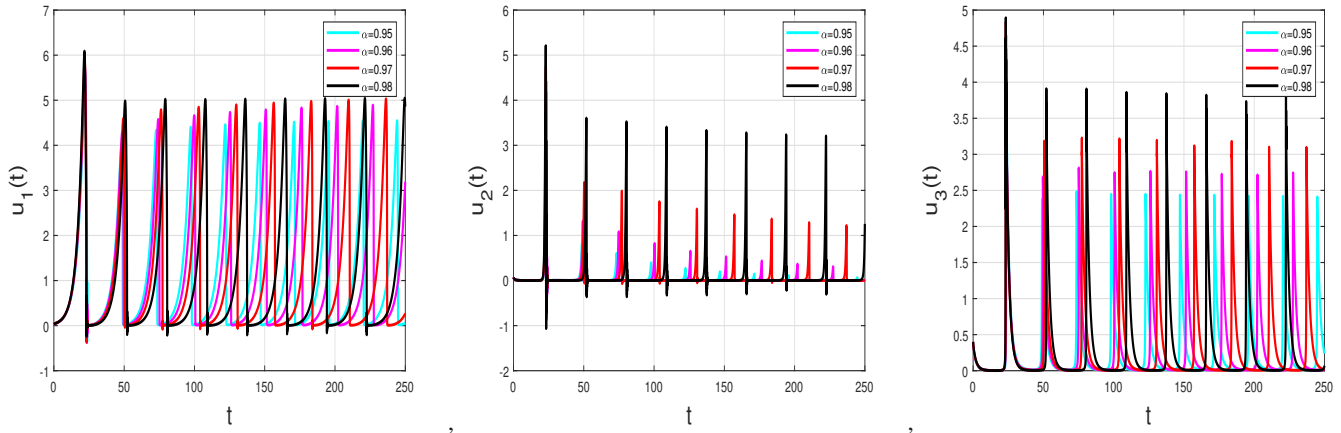


Fig. 13: Plot of solutions for different values of α with ICs $u_1(0) = 0.01, u_2(0) = 1.1$ and $u_3(0) = 0.05$ for $s_1 = 0.75, s_2 = 0.5, s_3 = 3.5, s_4 = 0.5, s_5 = 0.5, s_6 = 0.5$ and $s_7 = 1.5$.

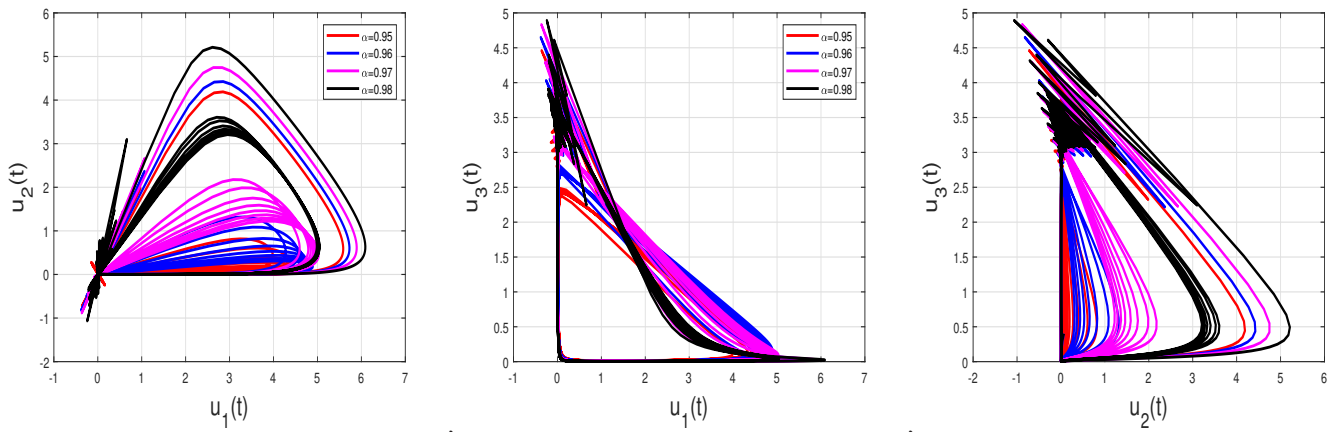


Fig. 14: 2D plot of solutions for different values of α with ICs $u_1(0) = 0.01, u_2(0) = 1.1$ and $u_3(0) = 0.05$ for $s_1 = 0.75, s_2 = 0.5, s_3 = 3.5, s_4 = 0.5, s_5 = 0.5, s_6 = 0.5$ and $s_7 = 1.5$.

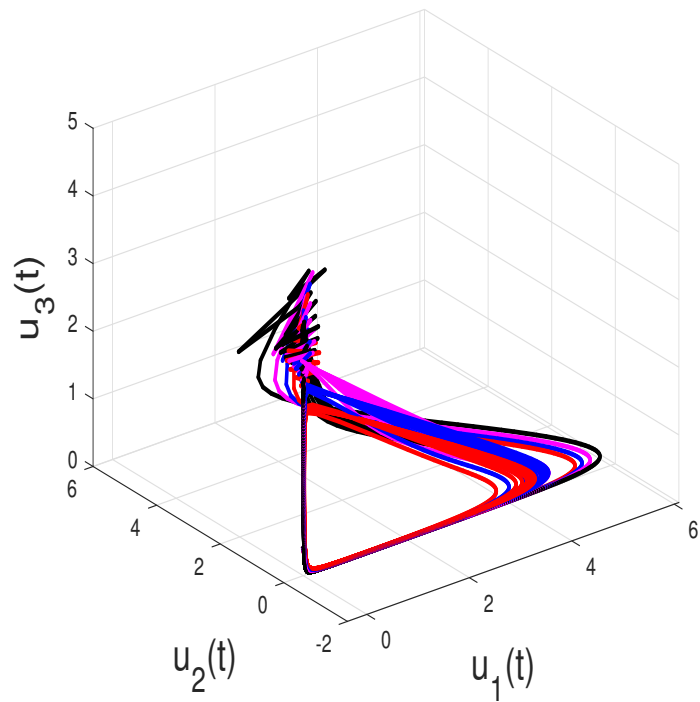


Fig. 15: Chaotic behaviour of of solutions for different values of α with ICs $u_1(0) = 0.01, u_2(0) = 1.1$ and $u_3(0) = 0.05$ for $s_1 = 0.75, s_2 = 0.5, s_3 = 3.5, s_4 = 0.5, s_5 = 0.5, s_6 = 0.5$ and $s_7 = 1.5$.

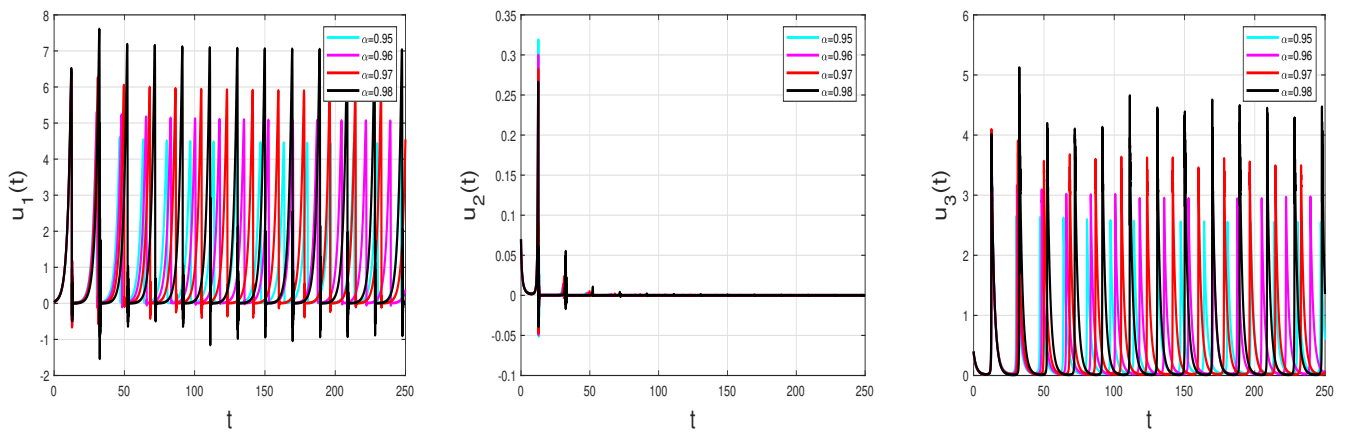


Fig. 16: Plot of solutions for different values of α with ICs $u_1(0) = 0.01, u_2(0) = 1.1$ and $u_3(0) = 0.05$ for $s_1 = 0.95, s_2 = 0.5, s_3 = 3.5, s_4 = 0.5, s_5 = 0.5, s_6 = 0.5$ and $s_7 = 1.5$.

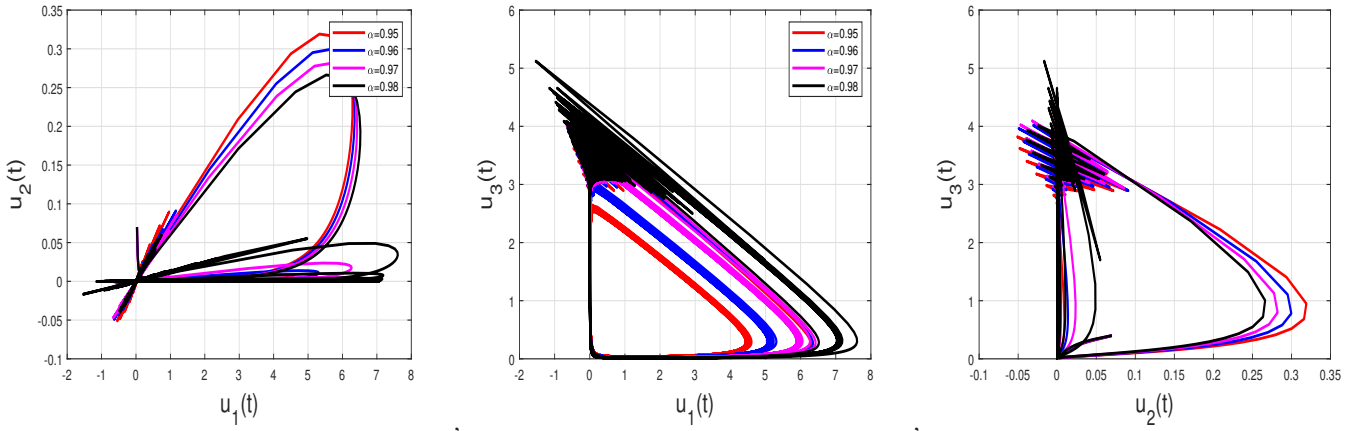


Fig. 17: 2D plot of solutions for different values of α with initial conditions $u_1(0) = 0.01, u_2(0) = 1.1$ and $u_3(0) = 0.05$ for $s_1 = 0.95, s_2 = 0.5, s_3 = 3.5, s_4 = 0.5, s_5 = 0.5, s_6 = 0.5$ and $s_7 = 1.5$.

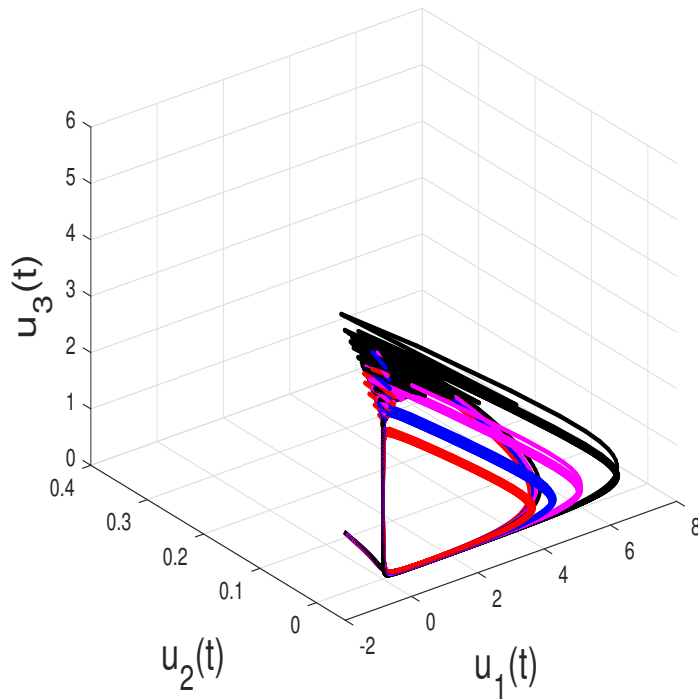


Fig. 18: Chaotic behaviour of solutions for different values of α with ICs $u_1(0) = 0.01, u_2(0) = 1.1$ and $u_3(0) = 0.05$ for $s_1 = 0.95, s_2 = 0.5, s_3 = 3.5, s_4 = 0.5, s_5 = 0.5, s_6 = 0.5$ and $s_7 = 1.5$.

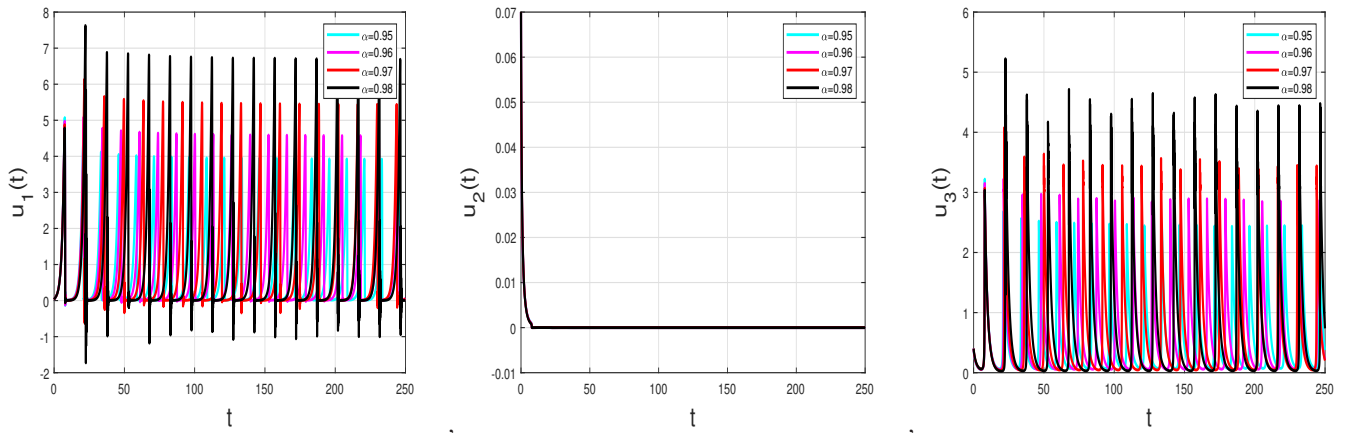


Fig. 19: Plot of solutions for different values of α with ICs $u_1(0) = 0.01, u_2(0) = 1.1$ and $u_3(0) = 0.05$ for $s_1 = 1.2, s_2 = 0.5, s_3 = 3.5, s_4 = 0.05, s_5 = 0.5, s_6 = 0.5$ and $s_7 = 1.5$.

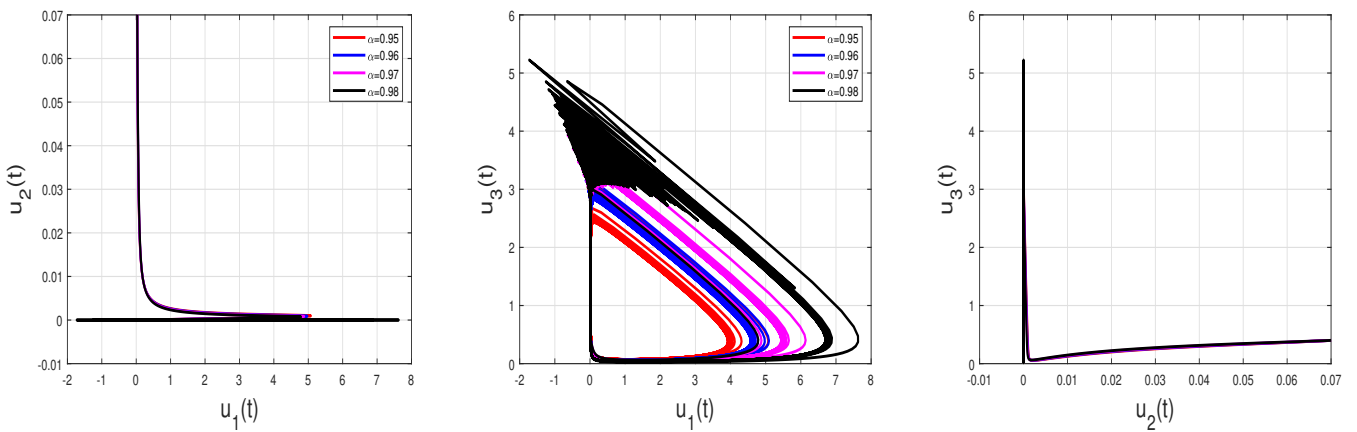


Fig. 20: 2D plot of solutions for different values of α with ICs $u_1(0) = 0.01, u_2(0) = 1.1$ and $u_3(0) = 0.05$ for $s_1 = 1.2, s_2 = 0.5, s_3 = 3.5, s_4 = 0.05, s_5 = 0.5, s_6 = 0.5$ and $s_7 = 1.5$.

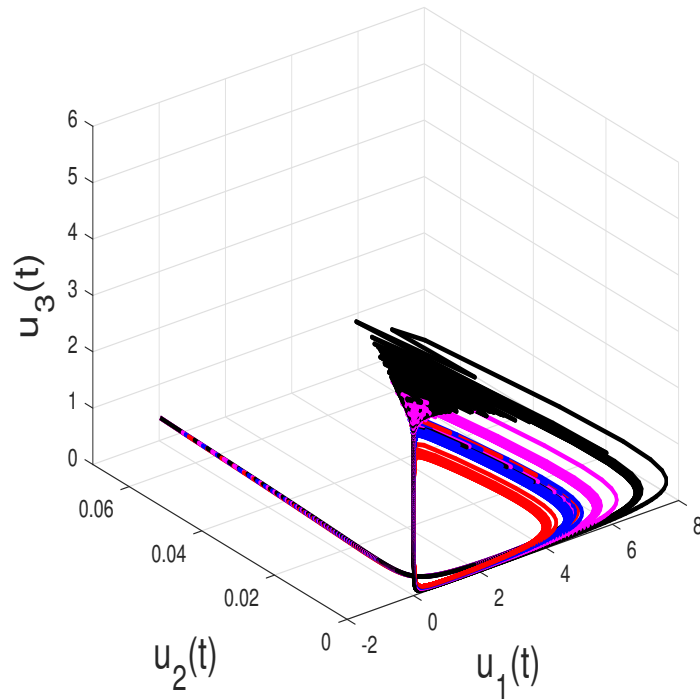


Fig. 21: Chaotic behaviour of of solutions for different values of α with ICs $u_1(0) = 0.01, u_2(0) = 1.1$ and $u_3(0) = 0.05$ for $s_1 = 1.2, s_2 = 0.5, s_3 = 3.5, s_4 = 0.05, s_5 = 0.5, s_6 = 0.5$ and $s_7 = 1.5$.

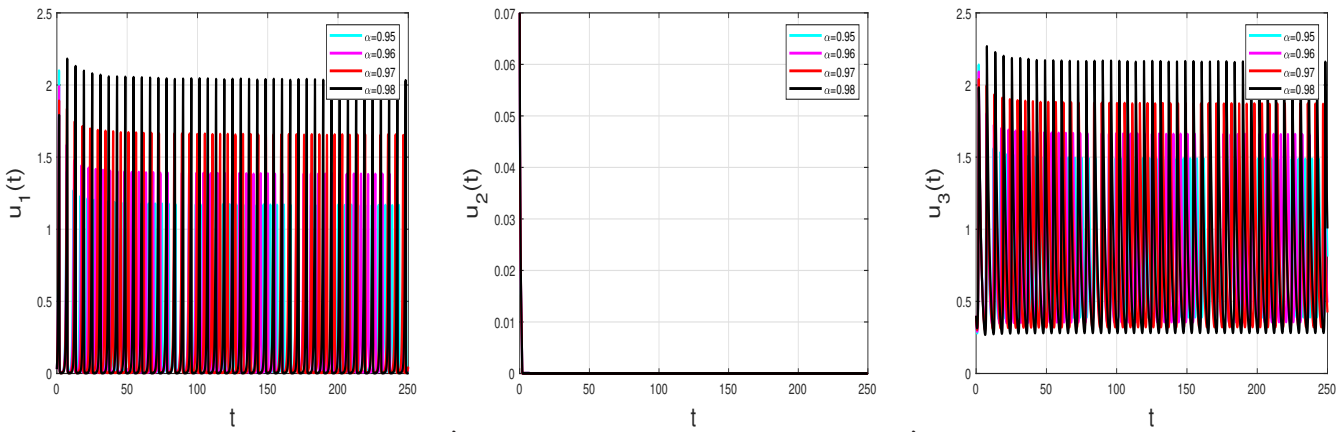


Fig. 22: Plot of solutions for different values of α with ICs $u_1(0) = 0.01, u_2(0) = 1.1$ and $u_3(0) = 0.05$ for $s_1 = 3.5, s_2 = 1.5, s_3 = 3.5, s_4 = 0.05, s_5 = 0.5, s_6 = 0.5$ and $s_7 = 1.5$.

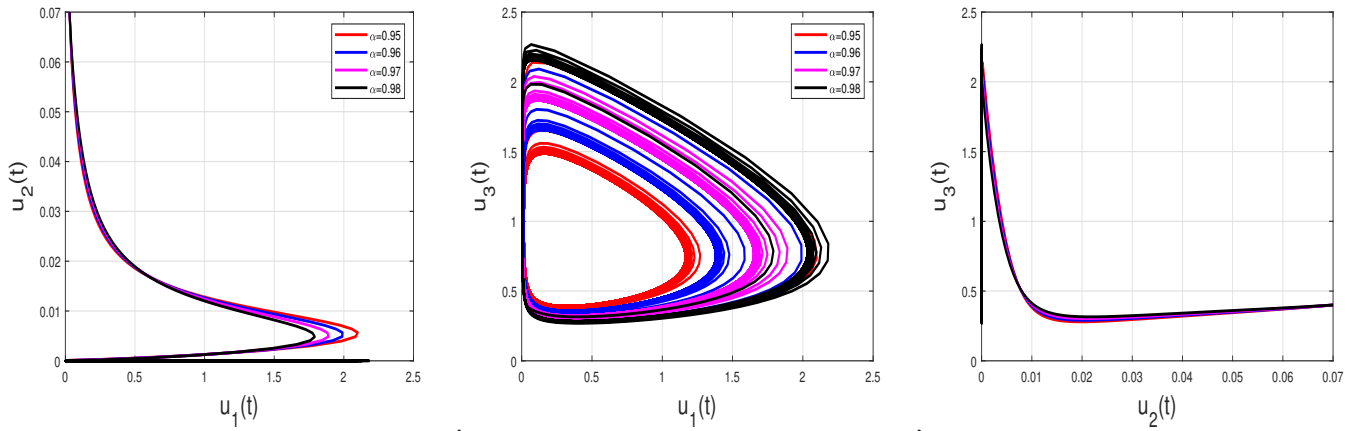


Fig. 23: 2D plot of solutions for different values of α with ICs $u_1(0) = 0.01, u_2(0) = 1.1$ and $u_3(0) = 0.05$ for $s_1 = 3.5, s_2 = 1.5, s_3 = 3.5, s_4 = 0.05, s_5 = 0.5, s_6 = 0.5$ and $s_7 = 1.5$.

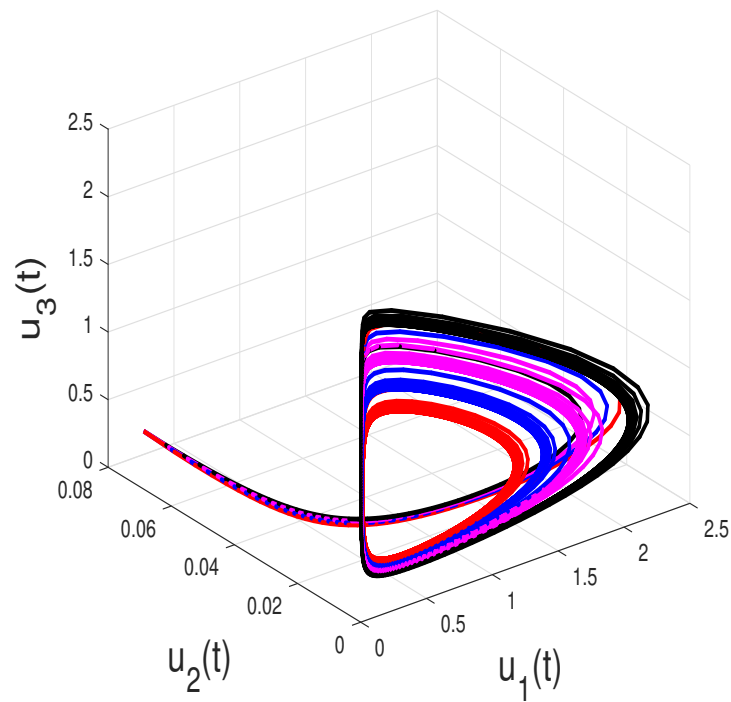


Fig. 24: Chaotic behaviour of of solutions for different values of α with ICs $u_1(0) = 0.01, u_2(0) = 1.1$ and $u_3(0) = 0.05$ for $s_1 = 3.5, s_2 = 1.5, s_3 = 3.5, s_4 = 0.05, s_5 = 0.5, s_6 = 0.5$ and $s_7 = 1.5$.

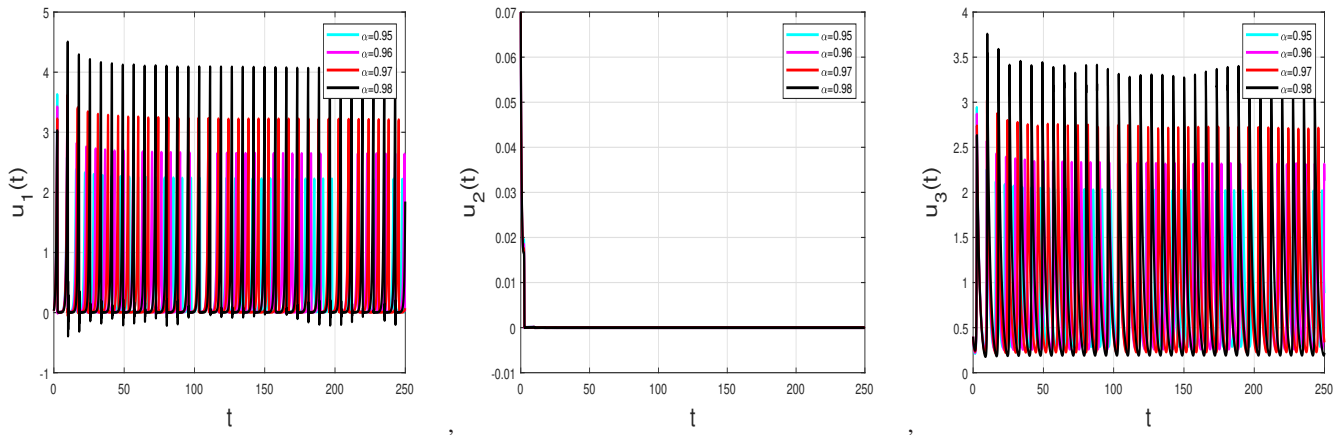


Fig. 25: Plot of solutions for different values of α with ICs $u_1(0) = 0.01, u_2(0) = 1.1$ and $u_3(0) = 0.05$ for $s_1 = 1.5, s_2 = 1.5, s_3 = 0.5, s_4 = 0.05, s_5 = 0.5, s_6 = 0.5$ and $s_7 = 0.5$.

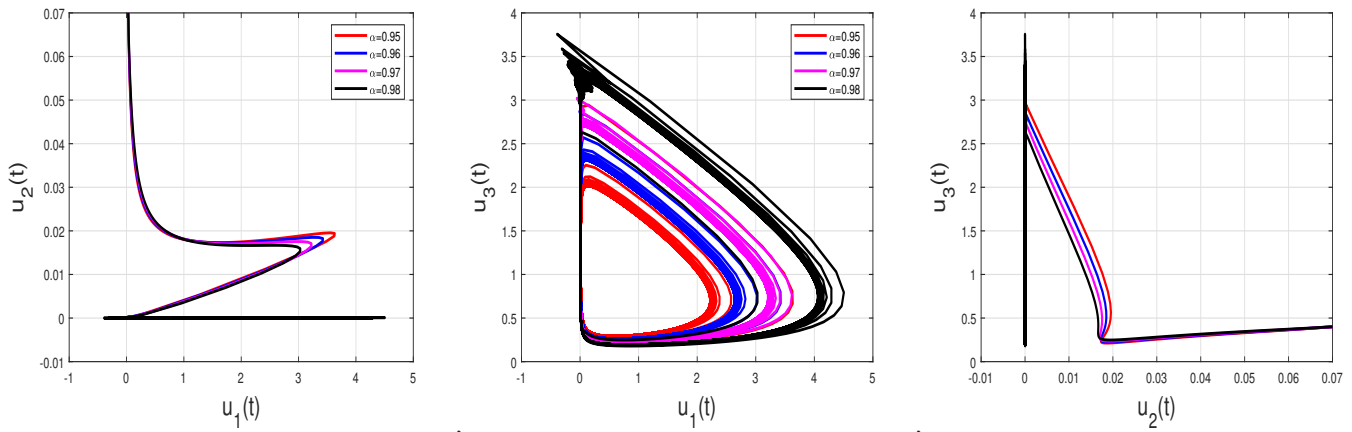


Fig. 26: 2D plot of solutions for different values of α with ICs $u_1(0) = 0.01, u_2(0) = 1.1$ and $u_3(0) = 0.05$ for $s_1 = 1.5, s_2 = 1.5, s_3 = 0.5, s_4 = 0.05, s_5 = 0.5, s_6 = 0.5$ and $s_7 = 0.5$.

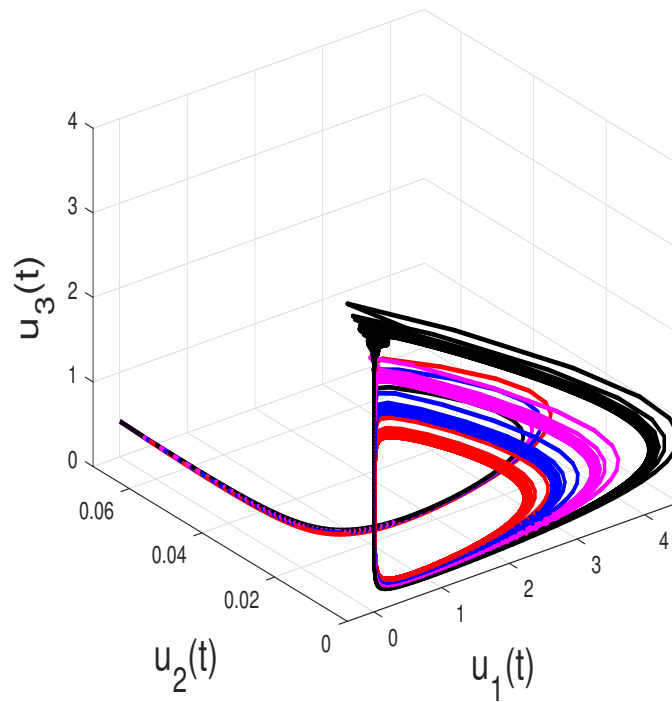


Fig. 27: Chaotic behaviour of of solutions for different values of α with ICs $u_1(0) = 0.01, u_2(0) = 1.1$ and $u_3(0) = 0.05$ for $s_1 = 1.5, s_2 = 1.5, s_3 = 0.5, s_4 = 0.05, s_5 = 0.5, s_6 = 0.5$ and $s_7 = 0.5$.

5 Conclusion

In this research study, numerical simulations of the Prey-Predator system is investigated using the ABC operator. We used the theorem of fixed-point to establish the occurrence and uniqueness of the results of the underlying system. Employing numerical approach, solutions of the system are produced that depict quite interesting dynamical features not possible to achieve under the classical approach of differential calculus. To understand the influence of fractional order α , numerical investigations are illustrated under engaging various fractional orders of α . To explain the chaotic behavior in deep, we have tried various values of the involved parameters in the model so that the state variables like susceptible prey, infected prey, and the predator populations could be visualized under ABC operator with different values of α . It may be noted that such detailed analysis under the ABC operator has not been previously encountered in the existing literature for the eco-epidemiological system. Future studies would include the analysis of the discussed system with another operator called the Caputo-Fabrizio operator and some optimal control theory would also be discussed in the realm of fractional calculus.

References

- [1] H. I. Freedman, *Deterministic mathematical models in population ecology*, Marcel Dekker, New York, USA, 1980.
- [2] J. D. Murray, *Mathematical biology*, Springer, Berlin, Germany, 2002.
- [3] B. Dubey and R. K. Upadhyay, Persistence and extinction of one-prey and two-predator system, *Nonlin. Anal. Model. Cont.* **9**(4), 307–329 (2004).
- [4] S. Gakkhar, B. Singh and R. K. Naji, Dynamical behavior of two predators competing over a single prey, *BioSys.* **90**(3), 808–817 (2007).
- [5] T. K. Kar and A. Batabyal, Persistence and stability of a two prey one predator, *Int. J. Eng. Sci. Tech.* **2**(2), 174–190 (2010).
- [6] G. P. Samanta, Analysis of a delay non-autonomous predator-prey system with disease in the prey, *Nonlin. Anal. Model. Cont.*, **15**(1), 97–108 (2010).
- [7] W. Wang and L. Chen, A predator-prey system with stage structure for predator, *Comp. Math. App.* **33**(8), 83–91 (1997).
- [8] O. Bernard and S. Souissi, Qualitative behavior of stages structure d p opulations : application to structural validation, *J. Math. Bio.* **37**(4), 291–308 (1998).
- [9] X. Zhang, L. Chen and A. U. Neumann, The stage-structured predator-prey model and optimal harvesting policy, *Math. Biosci.* **168**(2), 201–210 (2000).
- [10] J. Cui, L. Chen and W. Wang, The effect of dispersal on population growth with stage-structure, *Comp. Math. App.* **39**(1-52), 91–102 (2000).
- [11] J. Cui and Y. Takeuchi, A predator-prey system with a stage structure for the prey, *Math. Comp. Model.* **44**(11-12), 1126–1132 (2006).
- [12] S. Liu and E. Beretta, A stage-structured predator-prey model of Beddington-DeAngelis type, *SIAM J. Appl. Math.* **66**(4), 1101–1129 (2006).
- [13] J. Chattopadhyay and O. Arino, A predator-prey model with disease in the prey, *Nonlin. Anal.* **36**, 747–766 (1999).
- [14] K. P. Hadeler and H. I. Freedman, Predator-prey populations with parasitic infection, *J. Math. Biol.* **27**, 609–631 (1989).
- [15] L. Han, Z. Ma and H. W. Hethcote, Four predator prey models with infectious diseases, *Math. Comput. Model.* **34**(7–8), 849–858 (2001).
- [16] X. Zhou, J. Cui, X. Shi et. al. A modified Leslie-Gower predator-prey model with prey infection, *J. Appl. Math. Comput.* **33**, 471–487 (2010).
- [17] N. H. Sweilam, M. M. Khader and A. M. Nagy, Numerical solution of two- sided space-fractional wave equation using finite difference method, *J. Comput. Appl. Math.* **235**, 2832–2841 (2011).
- [18] J. Duarte, C. Januario, N. Martins and J. Sardanyes, Chaos and crises in a model for cooperative hunting a symbolic dynamics approach, *Chaos* **19**(4), 043102 (2009).
- [19] F. Capone, M.F. Carfora, R. De Luca and I. Torricollo, Turing patterns in a reaction-diffusion system modeling hunting cooperation, *Math. Comput. Simul.* **165**, 172–180 (2019).
- [20] C. Cosner, D. DeAngelis, J. Ault and D. Olson, Effects of spatial grouping on the functional response of predator, *Theor. Popul. Biol.* **56**(1), 65–75 (1999).
- [21] S. Pal, N. Pal, S. Samanta and J. Chattopadhyay, Effect of hunting cooperation and fear in a predator-prey model, *Ecol. Complex.* **39**, 100770 (2019).
- [22] K. Ryu and W. Ko, Asymptotic behavior of positive solutions to a predator-prey elliptic system with strong hunting cooperation in predators, *Physica A* **531**, 121726 (2019).
- [23] D. Sen, S. Ghorai and S. M. Banerjee, Allee effect in prey versus hunting cooperation on predator - enhancement of stable coexistence, *Int. J. Bifurc. Chaos* **29**(6), 1950081 (2019).
- [24] T. Singh, R. Dubey and V. N. Mishra, Spatial dynamics of predator-prey system with hunting cooperation in predators and type I functional response, *AIMS Math.* **5**, 673–684 (2020).
- [25] D. Song, Y. Song and C. Li, Stability and turing patterns in a predator-prey model with hunting cooperation and Allee effect in prey population, *Int. J. Bifurc. Chaos* **30**(09), 2050137 (2020).

- [26] D. Wu and M. Zhao, Qualitative analysis for a diffusive predator-prey model with hunting cooperative, *Physica A* **515**, 299—309 (2019).
- [27] S. Yan, D. Jia, T. Zhang and S. Yuan, Pattern dynamics in a diffusive predator-prey model with hunting cooperations, *Chaos Soliton. Fract.* **130**, 109428 (2020).
- [28] M. Yavuz and N. Sene, Stability analysis and numerical computation of the fractional predator—prey model with the harvesting rate, *Fractal Fract.* **4**(3), 35 (2020).
- [29] M. S. Hashemi, M. Parto-Haghighi and M. Bayram, On numerical solution of the time-fractional diffusion-wave equation with the fictitious time integration method, *Eur. Phys. J. Plus* **134**(10), 488.
- [30] M. Inc, M. Parto-Haghighi, M.A. Akinlar and Y.M. Chu, New numerical solutions of fractional-order Korteweg-de Vries equation, *Res. Phys.* **19**, 103326.
- [31] M. Inc, M. Partohaghighi, M. A. Akinlar, P. Agarwal and Y. M. Chu, New solutions of fractional-order Burger-Huxley equation, *Res. Phys.* **18**, 103290.
- [32] M. Partohaghighi, M .Inc, D. Baleanu and S. P. Moshoko, Fictitious time integration method for solving the time fractional gas dynamics equation, *Thermal Sci.* **23** (Suppl. 6), 2009–2016.
- [33] F. Jarad, T. Abdeljawad and Z. Hammouch, On a class of ordinary differential equations in the frame of Atangana–Baleanu fractional derivative, *Chaos Soliton. Fract.* **117**, 16–20 (2018).
- [34] S. Samko, A. Kilbas and O. Marichev, *Fractional Integrals and derivatives: theory and applications*, Gordon and Breach, Amsterdam, 1993.
- [35] A. Atangana and D. Baleanu, New fractional derivatives with non-local and nonsingular kernel: theory and application to heat transfer model, *Thermal Sci.* **20**, 763–769.
- [36] N. Aguila-Camacho, M.A. Duarte-Mermoud and J.A. Gallegos, Lyapunov functions for fractional order systems, *Commun. Nonlin. Sci. Numer. Simul.* **19**, 2951—2957 (2014).
- [37] Y. Li, Y. Chen and I. Podlubny, Stability of fractional-order nonlinear dynamic systems: Lyapunov direct method and generalized Mittag–Leffler stability, *Comput. Math. Appl.* **59**, 1810–1821 (2010).
- [38] M. Toufik and A. Atangana, New numerical approximation of fractional derivative with non-local and non-singular kernel: application to chaotic models, *Eur. Phys. J. Plus* **132**, 444 (2017).
-